

Rapidity correlations in 800 GeV proton-nucleus interactions

Namrata, Ashutosh Bhardwaj, Kirti Ranjan, Sudeep Chatterji, Ajay K. Srivastava, and R.K. Shivpuri^a

Centre for Detector and Related Software Technology, Department of Physics and Astrophysics University of Delhi, Delhi 110 007, India

Received: 30 March 2001 / Revised version: 3 August 2001

Communicated by Th. Walcher

Abstract. Rapidity correlations in 800 GeV proton interactions with emulsion nuclei are investigated for different targets and multiplicity regions. To study the energy dependence, the results have been compared with proton interactions at 200 GeV and 400 GeV. A common feature of all the interactions is the existence of strong, short-range correlations. However, no dependence of cluster parameters on primary energy or target mass is found. A marginal increase of correlation strength with multiplicity is observed.

PACS. 13.85.-t Hadron-induced high- and super-high-energy interactions (energy > 10 GeV) – 13.85.Hd Inelastic scattering:many-particle final states

1 Introduction

The existence of two-particle, short-range correlations is fairly well established in hadronic interactions at high energies [1], and several authors have suggested that there is independent cluster production due to these correlations. The dynamical significance of clusters is shown [2] by the “universality” of two-particle correlations at different primary energies for different projectiles. Most of the events studied are hadron-hadron interactions and no detailed work has been reported on hadron-nucleus interactions. It would be interesting to investigate how the target mass induces modifications, if any, with respect to the characteristics of clusters produced in the interactions. The dependence of cluster characteristics on multiplicity has also been investigated. Multiplicity is an interesting parameter for two reasons. Firstly, its value can be precisely determined. Secondly, its value can reflect the momentum transfer in an interaction. In the present work, we have investigated correlations among the secondary particles for proton-nucleus interactions at 800 GeV, which is the highest energy for fixed targets. Nuclear emulsion offers H, CNO and AgBr nuclei as targets. We can broadly classify the interactions as belonging to the H or CNO group of nuclei. However, events belonging to AgBr can be unambiguously identified. The unique advantage of nuclear emulsion lies in its high spatial resolution which allows resolution of tracks as close as $1\mu\text{m}$. We have exploited these characteristics of nuclear emulsion to investigate the cluster characteristics in proton-nucleus interactions.

We have investigated the dependence of cluster parameters on the target size (H, CNO and AgBr) as well

as on multiplicity. The present work has been carried out using an approach based on two-particle rapidity gap distribution, as suggested earlier [2]. We have compared our results with those at 200 GeV and 400 GeV, thus allowing us to determine the energy dependence of cluster parameters. We have also determined the normalized two-particle correlation function; the quantity which compares the two-particle distribution for the inclusive reactions $ab(1,2)$ with the product of the single-particle distributions for $ab(1)$ and $ab(2)$. This has been done for targets such as nucleon, CNO, AgBr and all emulsion nuclei. The total number of interactions is 3390, yielding a total number of shower particles of 62749. This represents the highest statistics reported so far in an emulsion experiment at 800 GeV.

2 Experimental details

A stack of 40 Ilford G5 emulsion pellicles of dimension $10 \times 8 \times 0.06\text{cm}^3$ was exposed to a proton beam of energy 800 GeV at Fermilab. The beam flux was 8.7×10^4 particles/cm². The scanning of the interactions was done under the $40\times$ objective of high-resolution microscopes by the area scanning method. The scanning efficiency, for each observer, was calculated using the double-scan data and the overall efficiency was found to be 99%. All the interactions were followed back, in order to ensure that they are due to beam track only. The interactions lying within $25\mu\text{m}$ each from the air and glass surface have not been considered for measurement. Taking these criteria into account, the total number of primary interactions was found to be 3390. All the measurements were

^a e-mail: hep@iasdl01.vsnl.net.in

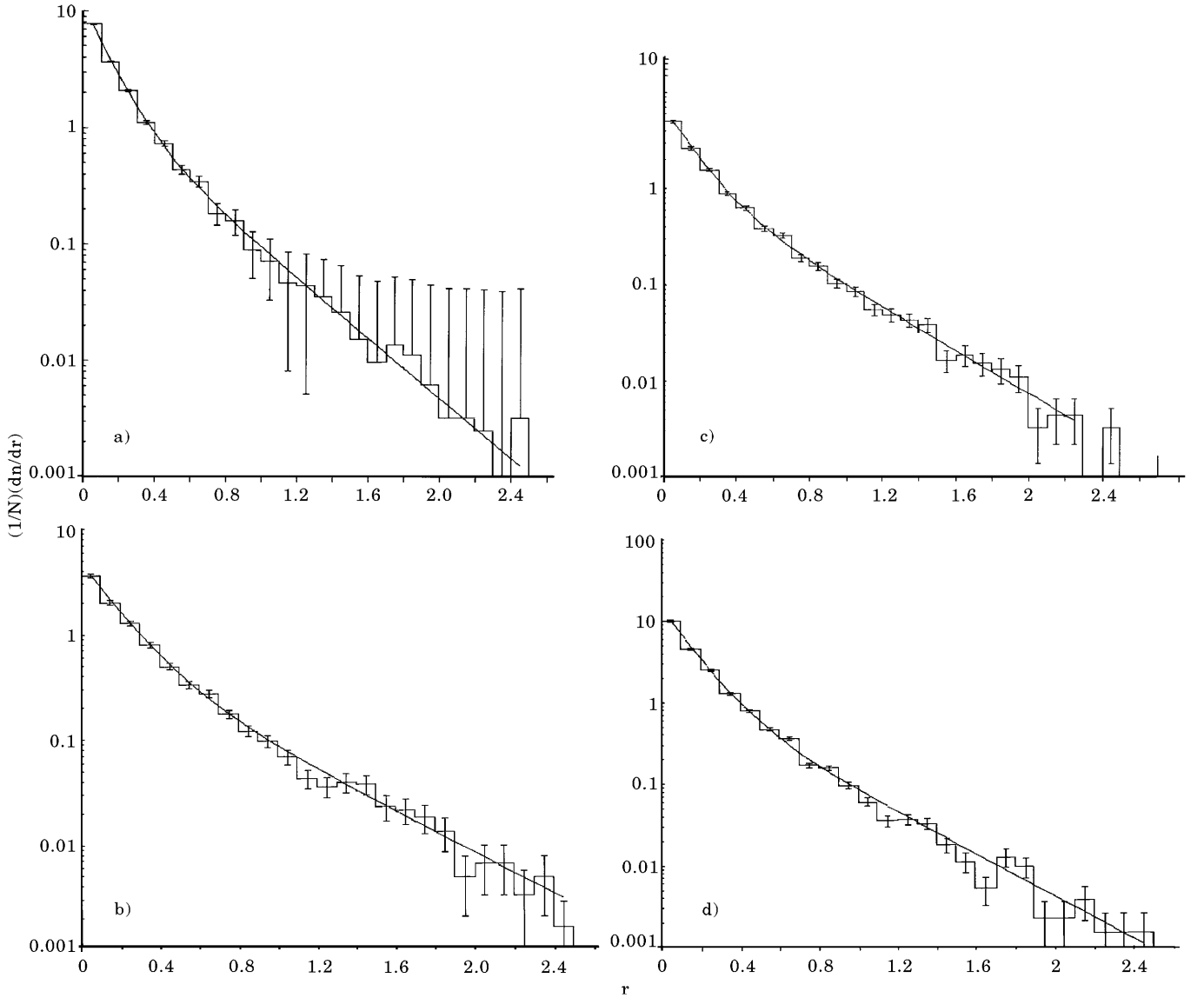


Fig. 1. Rapidity gap distribution of two adjacent charged particles for (a) proton-nucleus interactions, (b) proton-nucleon interactions, (c) proton-CNO interactions, (d) proton-AgBr interactions.

done under a $100\times$ oil immersion objective. Following the usual emulsion terminology, the secondary particles having ionisation $I \leq 1.4I_0$ and $I > 1.4I_0$ were designated as shower and heavy tracks and designated as N_s and N_h , respectively. I_0 is the ionisation of the primary particle. The space angle (θ) and the azimuthal angle (ϕ) of the shower tracks with respect to beam tracks were measured by the co-ordinate method. The values of x , y and z co-ordinates at the vertex and two points each on the shower and beam were measured and their angles were calculated. The uncertainty in angle measurement was 8×10^{-4} radians. The basic parameter which reflects the correlations, is the pseudorapidity (η) of shower particles which is given by

$$\eta = -\ln[\tan(\theta/2)], \quad (1)$$

and it is a good approximation to rapidity for very high energies. Pseudorapidity, hereinafter, will be referred to as rapidity. Shower particles with the largest and the smallest value of rapidity in an event were not considered, as such particles could be due to primary and target nuclei. We are interested in investigating the characteristics of produced particles only.

It has been shown [3] that the target nucleus can be broadly identified on the basis of value of N_h , as N_h reflects the number of nucleons of the target nucleus that have participated in the interaction. The interactions having $N_h \leq 1$, $2 \leq N_h \leq 5$ and $N_h \geq 9$ can be assumed to belong to nucleon, CNO and AgBr targets, respectively. The interactions with $N_h \leq 1$ are either due to collisions with pure H nuclei or due to the interactions with a single nucleon of the emulsion nuclei wherein the rest of the nucleus remains a spectator during the collision. The shower parti-

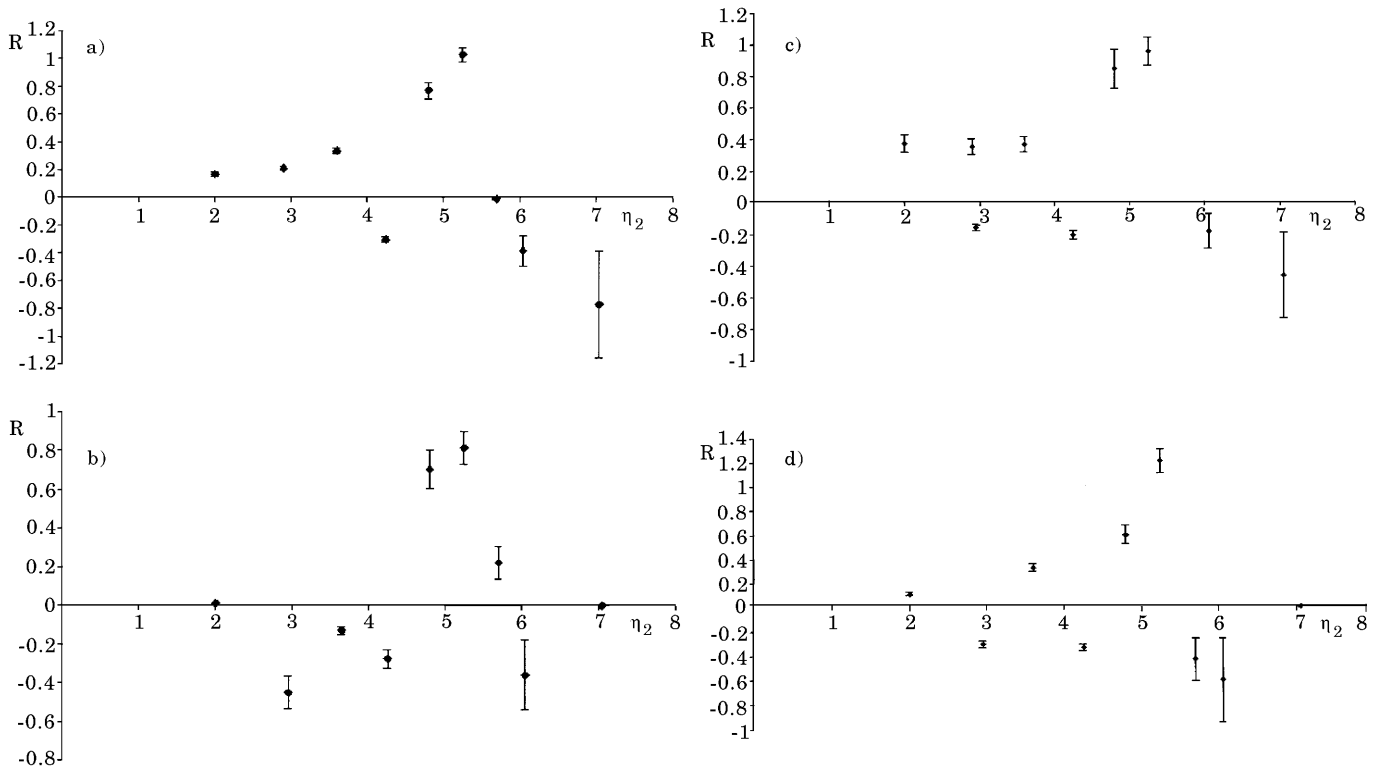


Fig. 2. Correlation function $R(\eta_1, \eta_2)$ as a function of η_2 when η_1 is fixed at a certain value for (a) proton-nucleus interactions, (b) proton-nucleon interactions, (c) proton-CNO interactions, (d) proton-AgBr interactions. The value of η_1 used is 5.25.

cle production takes place only in the elementary proton-nucleon collision. The interactions with $2 \leq N_h \leq 5$ were considered to belong mostly to proton-light nuclei (CNO) interactions. The interactions with $6 \leq N_h \leq 8$ are not considered here as they could be from collisions with light nuclei as well as with heavy nuclei. The interactions with $N_h \geq 9$ are unambiguous interactions with AgBr nuclei.

3 Results and discussion

A two-particle correlation necessarily implies that a rapidity gap distribution between two adjacent particles with rapidity η_1 and η_2 must have a sharp peak at small values of the rapidity gap ($r = \eta_1 - \eta_2$). Using the multiperipheral model, which describes the two-particle correlation and the rapidity gap distributions for the non-diffractive events, Snider [4] has fitted the experimental data by a distribution of the form

$$\frac{dn}{dr} = A \exp[-Br] + C \exp[-Dr]. \quad (2)$$

The rapidity distributions provide important information about the independent cluster emission. The analysis has been performed in all of the available pseudorapidity phase space. It has been shown earlier [5] that the parameter B reflects the strength of short-range correlations. We study below the correlations as a function of the target mass, primary energy and multiplicity of the interactions.

3.1 Variation with target mass

Figure 1 shows the rapidity gap (r) distribution for two adjacent particles. Thus, only those values which are closest to each other in rapidity space contribute to the values of r . It is clear from fig. 1(a) that the rapidity gap distribution of the two adjacent charged particles for proton-nucleus interactions (N_h -all) behaves exactly as predicted by the theoretical curve given by eq. (2). The values of parameters A , B , C and D are given in table 1 for p-A events. Figures 1(b), (c), and (d) show the rapidity-gap distribution of two adjacent charged particles for proton-nucleon, proton-CNO and proton-AgBr events, respectively. The following rapidity-gap distributions have been found to fit the data for interactions due to nucleon, CNO and AgBr nuclei, respectively:

$$\begin{aligned} \frac{dn}{dr} &= 2.92 \exp[-6.25r] + 0.67 \exp[-2.25r], \\ \frac{dn}{dr} &= 3.85 \exp[-7.48r] + 1.13 \exp[-2.58r], \\ \frac{dn}{dr} &= 8.61 \exp[-8.15r] + 1.37 \exp[-2.99r]. \end{aligned} \quad (3)$$

The fitting was done using the CERN Minuit programme. Taking into account the errors in values of B (as indicated in table 1), we find that B has a slightly higher value for AgBr as compared to nucleon targets. In the present work, the distributions whose parameters are given in table 1 show values of $\chi^2/\text{DOF} \sim 1$, when compared with the experiment.

Table 1. Values of the parameters A , B , C and D for proton-nucleon (pN) and proton-nucleus (pA) interactions at 200 GeV, 400 GeV and 800 GeV (pA interactions have been separated for CNO and AgBr targets at 800 GeV in the present work).

Event type	Energy (GeV)	Parameters				Ref.
		A	B	C	D	
p-n	200	2.40	3.10	0.20	0.90	[4]
	400	2.98	3.90	0.18	0.70	[8]
	800	2.92 ± 0.12	6.25 ± 0.25	0.67 ± 0.03	2.25 ± 0.09	present work
p-A	200	1.51 ± 0.22	5.27 ± 0.63	0.58 ± 0.22	2.38 ± 0.10	[7]
	400	2.49 ± 0.17	7.69 ± 0.52	0.93 ± 0.18	2.58 ± 0.08	
	800	6.10 ± 0.12	8.28 ± 0.16	1.54 ± 0.03	2.97 ± 0.06	present work
p-CNO	800	3.85 ± 0.13	7.48 ± 0.25	1.13 ± 0.04	2.58 ± 0.09	present work
p-AgBr	800	8.61 ± 0.23	8.15 ± 0.23	1.37 ± 0.04	2.99 ± 0.08	present work

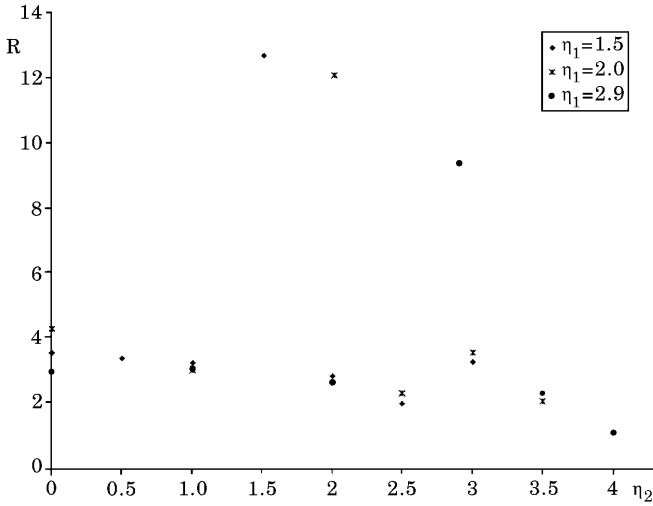


Fig. 3. Correlation function $R(\eta_1, \eta_2)$ as a function of η_2 when η_1 is fixed at a certain value for proton-nucleus interactions. Values of η_1 used are 1.5, 2.0 and 2.9.

We have also studied the two-particle correlations using the following correlation function [6]:

$$R(\eta_1, \eta_2) = \frac{\frac{1}{\sigma_{in}} \frac{d^2\sigma}{d\eta_1 d\eta_2} - \frac{1}{\sigma_{in}^2} \frac{d\sigma}{d\eta_1} \frac{d\sigma}{d\eta_2}}{\frac{1}{\sigma_{in}^2} \frac{d\sigma}{d\eta_1} \frac{d\sigma}{d\eta_2}} = \frac{N_T N_2(\eta_1, \eta_2)}{N_1(\eta_1) N_1(\eta_2)} - 1, \quad (4)$$

where, N_T is the total number of non-diffractive events, $N_1(\eta_1)$, $N_1(\eta_2)$ are the number of charged secondaries at η_1 and η_2 , respectively, and $N_2(\eta_1, \eta_2)$ is the number of pairs of tracks with η_1 and η_2 values.

The correlation function $R(\eta_1, \eta_2)$ is dimensionless and should be zero if particles are not correlated. Short-range correlation means that $R(\eta_1, \eta_2)$ is non zero when $\eta_1 = \eta_2$ and goes to zero for large separations ($\eta_1 - \eta_2$). The values of $R(\eta_1, \eta_2)$ are determined as a function of η_2 when $\eta_1 = 5.25$. R is plotted in fig. 2(a), (b), (c), (d), for all values of N_h , and for $N_h \leq 1$, $2 \leq N_h \leq 5$ and $N_h \geq 9$ events, respectively. The value of $\eta_1 = 5.25$ is chosen since

at this value, the number of tracks is quite large, thus reducing statistical error. In order to see whether the same effects are observed at different values of η , we have plotted R vs. η_2 for $\eta_1 = 1.5$, 2.0, and 2.9 in fig. 3 for all values of N_h . It is seen that the peak is observed when $\eta_2 = \eta_1$, for all values of η_1 considered here. From our experimental results, one can observe that for large values of $\eta_1 - \eta_2$, the correlation is very small, but for small values of $\eta_1 - \eta_2$, the correlation is positive and very strong. Hence, we can conclude that in general, there is a strong tendency for particles to emerge preferentially with a small difference in rapidity.

3.2 Variation with multiplicity

The double exponentials that best fit the data for $N_s > 13$ and $N_s \leq 13$ are shown in fig. 4(a) and (b), respectively, and are given by

$$\frac{dn}{dr} = 7.75 \exp[-(8.39 \pm 0.18)r] + 2.15 \exp[-(3.43 \pm 0.07)r], \quad (5)$$

$$\frac{dn}{dr} = 0.97 \exp[-(6.56 \pm 0.19)r] + 0.82 \exp[-(2.22 \pm 0.06)r]. \quad (6)$$

Here, we have considered events with $N_s \leq 13$ and $N_s > 13$, as the number of events was approximately the same for the two cases. The average multiplicity for $N_s \leq 13$ and $N_s > 13$ is found to be 9.08 and 24.04, respectively. It is seen that the value of B shows a marginal increase for $N_s > 13$ events. This increase may be due to larger number of clusters produced in such interactions. With increase in number of clusters, the probability that some of them may exhibit very strong correlations also increases, thus leading to an overall increase in the value of B .

3.3 Variation with primary energy

Table 1 shows the values of the parameters A , B , C and D for primary energies of 200 [7], 400 [8] and 800 GeV.

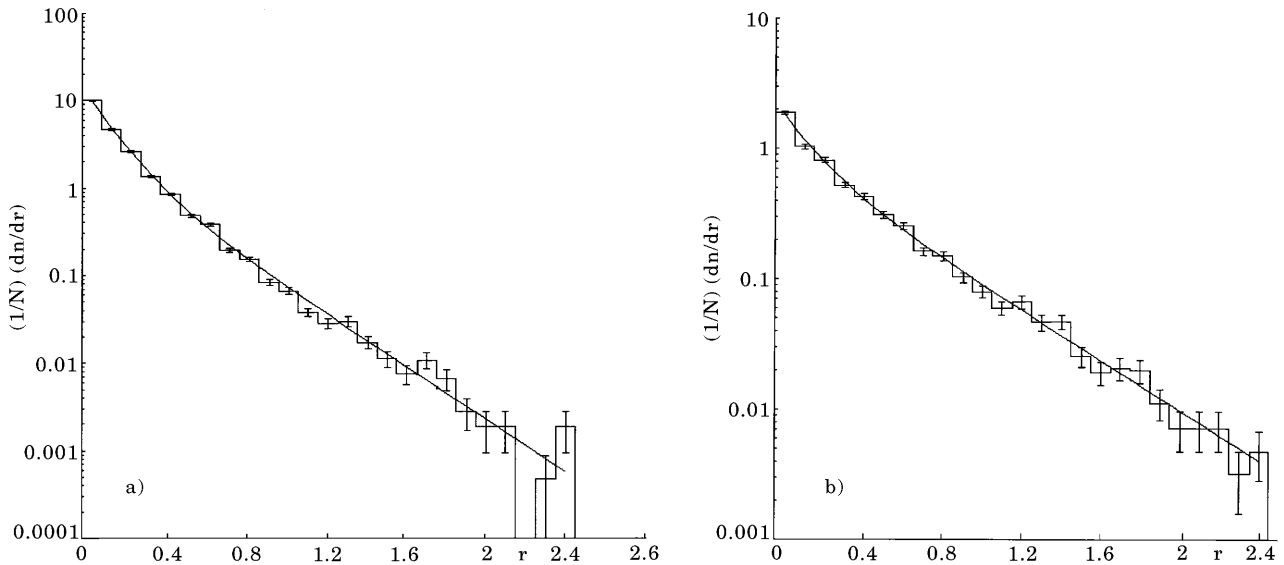


Fig. 4. Rapidity gap distribution of two adjacent charged particles for (a) $N_s > 13$, (b) $N_s \leq 13$.

Amongst all the parameters, only the parameter B is of crucial significance, since its magnitude reflects the strength of correlations. No significant dependence of parameter B on the primary energy is observed in p-A interactions, while in proton-nucleon interactions an energy dependence might be present. Thus, the correlations are independent of the primary energy. In an earlier work [9], one of us (RKS) proposed a new approach based on two-particle rapidity distribution to study scaling. It is seen from table 1 that the values of parameters B and D for p-A interactions at 200, 400 and 800 GeV events are not significantly different from each other. Thus, the rapidity gap distributions approach energy-independent limits. The cluster parameters for nucleon targets for 200 and 400 GeV have not been provided with errors and hence, they cannot be compared with the present work.

4 Conclusions

The parameter B which measures the strength of correlation shows only a marginal increase with increase in multiplicity. However, it does not show any significant dependence on target mass or primary energy. The independence of correlations from target mass, ranging from nucleon to AgBr, shows that particle production takes place only after collision with a single nucleon and the rest of the nucleus remains a spectator during the production

process. The value of B remaining independent of primary energy shows the scaling behaviour of correlations. It would be interesting to investigate how the correlations behave at energies in the TeV region (CERN - LHC).

We are grateful to the Fermi National Accelerator Laboratory, Illinois, for exposure facilities at the Tevatron and to Dr. Ray Stefanski for help during exposure of the emulsion stack. We would like to thank Dr. R. Wilkes for processing facilities. Kirti Ranjan and Sudeep Chatterji would like to thank the Council for Scientific and Industrial Research, New Delhi, for financial support.

References

1. R. Slansky, Phys. Rep. C **11**, 99 (1974); L. Foa, Phys. Rep. C **22**, 1 (1975); S. Fredriksson et al., Phys. Rep. **144**, 187 (1987). Detailed references are given in the above papers.
2. R.K. Shivpuri, Phys. Rev. D **15**, 1926 (1977).
3. C. Gupt et al., Phys. Rev. D **26**, 2202 (1982).
4. D.R. Snider, Phys. Rev. D **11**, 140 (1975).
5. R.K. Shivpuri et al., Nuovo Cimento A **104**, 113 (1991).
6. Baroni et al., Nucl. Phys. B **103**, 213 (1976).
7. M.M. Agrawal et al., J. Phys. Soc. Jpn. **51**, 353 (1982).
8. Sengupta et al., Phys. Rev. D **20**, 601 (1979).
9. R.K. Shivpuri, Lett. Prog. Theor. Phys. **58**, 691 (1977); R.K. Shivpuri, Nuovo Cimento A **49**, 67 (1979); **73**, 295 (1983).